ISSN 0018-151X, High Temperature, 2017, Vol. 55, No. 2, pp. 199–208. © Pleiades Publishing, Ltd., 2017.
Original Russian Text © R.I. Nigmatulin, R.Kh. Bolotnova, 2017, published in Teplofizika Vysokikh Temperatur, 2017, Vol. 55, No. 2, pp. 206–215.

THERMOPHYSICAL PROPERTIES OF MATERIALS

Simplified Wide-Range Equations of State for Benzene and Tetradecane

R. I. Nigmatulin[a, b] and R. Kh. Bolotnova[b, *]

[a] *Shirshov Institute of Oceanology, Russian Academy of Sciences, Moscow, Russia*
[b] *Mavlyutov Institute of Mechanics, Ufa Scientific Center, Russian Academy of Sciences, Ufa, Russia*
**e-mail: Bolotnova@anrb.ru*

Received November 16, 2015

Abstract—The equations of state for benzene, tetradecane, and their deuterated counterparts are derived on the basis of the original method of constructing the wide-range equations of state for hydrocarbon liquids in an analytical form. The equations describe gas and liquid phases at intensive gas-dynamic processes with consideration of evaporation and condensation and include dissociation and ionization processes associated with super-high pressures and temperatures.

DOI: 10.1134/S0018151X17010151

INTRODUCTION

As was shown in the works devoted to the collapse of cavitation bubbles [1–3], a sufficiently high molecular mass (low speed of sound) of the source vapor is favorable for higher energy focus supply, owing to the formation of a converging shock microwave and preservation of a subspherical shape of the bubble due to a higher vapor density at its border. Such an energy focus leads to the formation of a nanosized (about 10^2 nm) plasmoid, in which an extreme temperature (about 10^8 K) and density (about 10 g/cm^3) are developed within a picosecond time interval (about 10^{-1} ps). Thermonuclear fusion reactions of the type D + D or D + T, where D and T are the nuclei of hydrogen isotopes, deuterium and tritium, are accomplished under these conditions. Upon increasing the molecular weight of the source vapor, the efficiency of these processes and such characteristics as the extreme zone size, its lifetime, and the thermonuclear reaction yield should grow as well. In this regard, liquids with a high molecular weight, in particular, heavy hydrocarbon liquids, are of special interest. For the analysis of the processes associated with the collapse of cavitation bubbles in such liquids, one needs their wide-range equations of state (EOS) in the range of temperatures from 300 to 10^8 K and densities from 10^{-3} to 10^4 kg/m^3, which include the liquid and vapor states, subcritical state, states of extremely high pressures of about 10^9 bar, and dense plasma state.

The results of experimental and theoretical studies and numerical simulation of thermophysical properties of substances are given in reviews [4–7], where it is also shown that the problems of thermal physics remain one of the key research directions. Issues related to the construction of wide-range EOS are also addressed in [4–7]. Up to now, a large number of EOS are proposed to describe the properties of liquids and gases. Multiparametric empirical EOS are basically used when comprehensive experimental data on the p–V–T dependences of the investigated substances are available. The above-mentioned EOS are particularly inaccurate when used to describe liquid-phase states at high pressures. Special EOS are developed for these purposes.

Based on experimental data and general theoretical notions, EOS models covering all aggregate states, including dense plasma, are developed in the physics of high pressures and temperatures [8]. Thermodynamics of these states is constructed within the semiempirical models, in which diverse experimental data are used for determining the numerical values of unrestricted coefficients selected in functional dependences of the potential in accordance with theoretical notions [8, 9]. Tabulated wide-range EOS [10] combine the accuracy of experimental and theoretical data, and continuity and smoothness of thermodynamic functions in which the thermal and elastic components of pressure and energy are given in tabular form.

Due to the advances in computer technology in recent decades, molecular dynamics simulation has been recognized as an effective tool in the study of thermodynamic properties of substances [7], which allows one to obtain a complete microscopic description of the processes occurring in materials and to study systems containing tens of millions of atoms. However, the applicability of this method for the study of properties of substances is limited by a system size of about 100 nm.

To date, fairly extensive experimental data on thermodynamic properties of the gaseous state of matter have been accumulated [11, 12]. In addition, data on the shock compression of hydrocarbons in the condensed phase are available [13].

Studies of highly intense gas dynamics processes accompanied by the collapse of cavitation bubbles, in which heavy hydrocarbon compounds are used as working fluids, are of high importance. Hence, the need in the construction of a relatively simple equations of state applicable in a broad range of pressure and temperature arises, taking into account the heat and mass transfer processes between liquid and gas phases in subcritical states, and under the conditions of extremely high pressures and temperatures, including dissociation and ionization.

Benzene (C_6H_6 and C_6D_6) and tetradecane ($C_{14}H_{30}$ and $C_{14}D_{30}$) are considered in this work as source liquids, for which universal EOS in analytic form are developed to describe the coexisting vapor and liquid phases with the use of an earlier developed technique [14, 15].

SIMPLIFYING ASSUMPTIONS USED FOR THE CONSTRUCTION OF EQUATIONS OF STATE FOR LIQUIDS AND GASES

To describe thermodynamic properties of normal and deuterated hydrogen-containing compounds in the gas and liquid phases, it is suggested to use the well-known Mie–Grünaisen EOS, which is expressed as a sum of the potential, thermal, and chemical components of the internal energy and pressure [16–19]:

$$p = p^{(p)} + p^{(T)}, \tag{1}$$

$$e = e^{(p)} + e^{(T)} + e^{(\mathrm{ch})}, \tag{2}$$

where p in Eq. (1) and the internal energy, e, in Eq. (2) are given as a sum of the potential (p), thermal (T), and chemical (ch) components. The chemical energy may change during phase transitions and chemical reactions. The potential component (cold part) is responsible for the intermolecular, interatomic, or interionic interactions and determined by the density of a substance, as follows:

$$p^{(p)} = p^{(p)}(\rho) = \rho^2\left(\frac{de^{(p)}}{d\rho}\right),$$
$$e^{(p)} = e^{(p)}(\rho) = \int_{\rho^\circ}^{\rho}\frac{p^{(p)}(\rho)}{\rho^2}d\rho. \tag{3}$$

The potential component of the pressure and energy, which characterizes the elastic interaction between atoms at temperature $T = 0$ K, is described by a potential of the Born–Mayer type, including intermolecular repulsive forces in the first term and attractive forces of a condensed medium in the second term [16, 17], as follows:

$$p^{(p)}(\rho) = A\left(\frac{\rho}{\rho_0}\right)^{-\beta+1}\exp\left[b\left(1-\left(\frac{\rho}{\rho_0}\right)^{-\beta}\right)\right]$$
$$- K\left(\frac{\rho}{\rho_0}\right)^{\xi+1}, \quad \rho = \frac{1}{V}, \quad e^{(p)}(\rho) = \int_{\rho^\circ}^{\rho}\frac{p^{(p)}(\rho)}{\rho^2}d\rho \tag{4}$$
$$= \frac{A}{\beta\rho_0 b}\exp\left[b\left(1-\left(\frac{\rho}{\rho_0}\right)^{-\beta}\right)\right] - \frac{K}{\xi\rho_0}\left(\frac{\rho}{\rho_0}\right)^{\xi} + e^\circ.$$

Here, A, K, b, ξ, and β are constants, and e° is the integration constant of the potential energy, at which a minimum value of the potential energy is achieved, following the formula $e^\circ = e^{(p)}(\rho^\circ) = 0$, where ρ° is the density of a liquid at zero elastic pressure ($p^{(p)}(\rho^\circ) = 0$).

The Born–Mayer potential was first suggested to describe the elastic behavior of metals, ionic crystals, and other condensed states of matter in shock waves. The behavior of liquids in the high-compression region subtly differs from the behavior of solids, and the Born–Mayer potential can also be applied here [20]. The expansion of the application area of this potential for large volumes is dictated by the need to describe the behavior of substances in the vapor and liquid phases in vapor–liquid systems, for example, when supercompression of vapor bubbles under the influence of acoustical waves on a liquid is simulated [1, 21].

The thermal component depends on the thermal motion of molecules, atoms, ions, and electrons. To determine the thermal components, the approximation is accepted, which follows from the thermodynamic identity,

$$T\xi_V(V,T) = p + \left(\frac{\partial e}{\partial V}\right)_T, \quad \xi_V(V,T) \equiv \left(\frac{\partial p}{\partial T}\right)_V. \tag{5}$$

Assuming the constancy of the heat capacity, c_V, and the dependence of the isochoric pressure coefficient, ξ_V, and, consequently, of the Grünaisen function, G, only on the volume from Eq. (5), the following relations can be obtained:

$$p^{(T)}(V,T) = \left(\frac{\partial p}{\partial T}\right)_V T$$
$$\equiv \xi_V(V)T = \frac{\mathrm{G}(V)c_V}{V}T, \quad e^{(T)} = c_V T. \tag{6}$$

Due to the lack of experimental data on deuterated compounds, the density and heat capacity were determined, taking into account the molecular weight ratio of a normal substance and its deuterated analogue.

LOW-PRESSURE REGION AND STATE AT THE SATURATION LINE

In the low-pressure region, when the vapor density, ρ, and the pressure, p, are not so high ($p < 10$ bar), the

Table 1. Parameters of EOS of the molecular phase

Parameter	Benzene		Tetradecane	
	C_6H_6	C_6D_6	$C_{14}H_{30}$	$C_{14}D_{30}$
M, kg/kmol	78	84	198	228
c_G, J/(kg K)	960.0	889.4	1580.0	1372.1
c_L, J/(kg K)	1194	1108.7	1670	1450.3
ρ_{L0}, kg/m^3	879	946.6	763	878.6
ρ_{cr}, kg/m^3	304	324.7	222	255.6
C_{0L}, m/s	1306	1258.5	1331	1240.4
$e_G^{(ch)}$, J/kg	1.1×10^5	1.3×10^5	0.36×10^5	0.62×10^5
e_m°, J/kg	0.409×10^6	0.380×10^6	0.356×10^6	0.309×10^6
ρ_L° / ρ_{L0}	1.265		1.181	
A_m, Pa	0.7×10^8		6.6×10^7	
b_m	27.225		31.2	
K_m, Pa	0.38×10^9		0.28×10^9	
ξ_m	1.2		1.1	
β_m	0.3333		0.3333	

gas parameters (ρ, p, T, and e) fit the ideal gas equation of state, $p = \frac{R}{M}\rho T$, where $R = 8.314$ J/(mol K) is the universal gas constant, and M is the molecular weight; in addition, the gases are characterized by the constant-volume heat capacity, c_G, and adiabatic index, γ_G, in the following way [11, 12]:

$$e = c_G T, \quad p = (\gamma_G - 1)c_G \rho T. \tag{7}$$

The heat capacities and densities of the gas and liquid under normal thermodynamic conditions and the critical parameters, p_{cr}, ρ_{cr}, and T_{cr} [22] are given in Tables 1 and 2. EOS of a vapor in the form of EOS for the ideal gas is inapplicable at higher pressures associated with the thermodynamics of a critical state, when pressure and temperature are close to their critical values. It is necessary to take into account the influence of intermolecular interactions on the properties of a vapor (as well as of a liquid) in the form of elastic potential energy and the dependence of the Grünaisen function on the density.

To evaluate the agreement between the calculated and experimental densities, $\rho_{LS}(p)$ and $\rho_{GS}(p)$, of the liquid and gas, respectively, at the saturation line, the Clausius–Clapeyron differential equation is applied [18]:

$$\frac{dT_S}{dp} = \frac{T_S(p)}{h_{LG}(p)}\left(\frac{1}{\rho_{LS}(p)} - \frac{1}{\rho_{GS}(p)}\right). \tag{8}$$

Based on the thermodynamic conditions of the consistency of the internal energies of a vapor and liquid on the saturation line, the following correction to the internal energy is derived [18]:

$$e_G(\rho_{GS}(T), T) = e_L(\rho_{LS}(T), T) + h_{LG}(T) - p_S(T)\left(\frac{1}{\rho_{GS}(T)} - \frac{1}{\rho_{LS}(T)}\right), \tag{9}$$

where $e_G(\rho_{GS}(T), T)$ and $e_L(\rho_{LS}(T), T)$ are the internal energy values for vapor and liquid at the saturation line.

The approximation temperature dependences of the saturation pressure, $p_S(T)$, and the heat of vaporization, $h_{LG}^*(T)$, which are proposed in the present work for the studied compounds, are in agreement with the experimental data [11, 22] and expressed as follows:

$$p_S(T) = p_* \exp\left(-\frac{T_1}{T - T_2}\right) + p_{**}\left(1 + \tanh\left(\frac{T - T_{cr}}{T_3}\right)\right), \tag{10}$$

$$h_{LG}^*(T) = h^*\left(1 - \frac{T}{T_{cr}}\right)^\kappa. \tag{11}$$

Table 2. Approximation parameters of the pressure, $p_S(T)$, and vaporization enthalpy, $h^*_{LG}(T)$, at the saturated vapor line

Parameter	Benzene	Tetradecane
p_{cr}, bar	49.2	15.7
p_*, bar	2.68×10^4	1.7×10^4
p_{**}, bar	–	0.54
T_{cr}, K	562.6	693.0
T_1, K	3450	4150
T_2, K	15	102
T_3, K	–	10
h^*, $(m/s)^2$	5.54×10^5	4.43×10^5
κ	0.34	0.38

The values of the approximation parameters, T_1, T_2, T_3, p_*, p_{**}, h^*, and κ, obtained in the present work for benzene and tetradecane are given in Table 2.

DISSOCIATION AND IONIZATION OF GAS/VAPOR

The dissociation and ionization processes are accompanied by the changes in the structure of a substance, which are associated with phase transitions, chemical reactions, etc. This leads to a change in the intermolecular forces, which are characterized by the potential pressure, $p^{(p)}(\rho)$, and the Grünaisen function, $G(\rho)$. Changes in the thermal motion of different atoms become independent, increasing the heat capacity, c, of a substance. Owing to the structural changes, the energy absorption takes place in a substance, which is taken into account by the chemical component, $e^{(ch)}$, of the internal energy.

To describe an intermediate state during the transition from the molecular (undissociated) to the atomic (dissociated) phase, a substance was considered as a mixture of two components, namely, molecular ($k = m$) and atomic ($k = d$) components, with different equations of state and additive or equal values of the pressure components, m and d, as follows:

$$\begin{gathered}\rho = \varphi_m\rho_m + \varphi_d\rho_d, \quad \varphi_m + \varphi_d = 1,\\ p = \varphi_m p_m(\rho_m, T) + \varphi_d p_d(\rho_d, T),\\ \text{or } p = p_m(\rho_m, T) = p_d(\rho_d, T),\\ e = x_m e_m(\rho_m, T) + x_d e_d(\rho_d, T),\\ x_m = \varphi_m\rho_m/\rho, \quad x_d = \varphi_d\rho_d/\rho,\\ e_k = e_k^{(p)}(\rho_k) + c_k T + e_k^{(ch)},\\ p_k = p_k^{(p)}(\rho_k) + \rho_k G_k(\rho_k) c_k T \ (k = m, d).\end{gathered} \tag{12}$$

Here, φ_d and x_d are the volume and mass fractions of a dissociated gas ($\varphi_m = 1 - \varphi_d$; $x_m = 1 - x_d$).

For the undissociated liquid and gas/vapor states, the Grünaisen coefficient was used in accordance with Eq. (6). All the other gas states (dissociated and ionized, $j = 1, \ldots, Z$) correspond to a mixture of monatomic gases. Depending on the initial molecular structure of the studied hydrocarbon compound, the mixture may consist of the atoms or ions of deuterium (D) or hydrogen (H), carbon (C), and electrons. Owing to the monoatomic structure, the adiabatic index in this case is as follows: $\gamma = G + 1 = 1.667$.

The specific heat capacity of a fully dissociated gas is expressed as $c_d = 3/2\, nk_B$, where $k_B = 1.38 \times 10^{-23}$ J/K is the Boltzmann constant, and n is the number of atoms and ions per unit mass of a gas. If assuming that the contribution of electrons to the heat capacity of all the ionized states is negligible due to the very short time of ionization (10^{-13}–10^{-10} s [16]), for example, arising from shock compression in the central zone of microbubbles upon cavitation collapse [21], then the Grünaisen coefficient and nonequilibrium heat capacity of ionized plasma (e.g., benzene) have the following values:

$$\begin{gathered}\text{H–benzene: } M(C_6H_6) = 78 \text{ kg/kmol},\\ G_d = 0.667, \quad c_d = 1780 \text{ J/(kg K)};\\ \text{D–benzene: } M(C_6D_6) = 84 \text{ kg/kmol},\\ G_d = 0.667, \quad c_d = 1652.9 \text{ J/(kg K)}.\end{gathered} \tag{13}$$

The values of the nonequilibrium heat capacities of benzene and tetradecane are shown in Table 3. The intermediate stage of the transition of the heat capacity from the molecular liquid and gaseous phases to the dissociated and ionized states is determined by the kinetics of the phase transition and by the conditions of the dissociation process simulated with the assumption of a nonequilibrium scheme.

The chemical part of the internal energy for the gas/vapor phase was calculated taking into account the evaporation/condensation heat, $e_m^{(ch)}$, dissociation energy, $e_d^{(ch)}$, and ionization energy, $e_i^{(ch)}$, of a molecule. The chemical energy depends on the ionization level, x_j, of all types of electron excitation ($j = 1, 2, \ldots, Z$) and corresponds to the chemical energies (ionization potentials), $e_j^{(ch)}$, of all the atoms in a molecule [23].

The energy required for the complete dissociation of a gas is calculated in two steps. At the first step, the relative energy, Q_m, given per unit mol of a substance and required for the dissociation of the molecules into the C atoms and H_2 molecules is determined. It was assumed at this point that the relative dissociation energies of the molecules of D- and H-gases are the same. At the second step, the energies of the dissociation of H_2 (D_2) into two H (D) atoms (Q_{H_2} or Q_{D_2}), reduced to unit mol of hydrogen (deuterium), were found by using [24]:

Table 3. Constants of EOS of the dissociated and ionized phases

Constant	Benzene		Tetradecane	
	C_6H_6	C_6D_6	$C_{14}H_{30}$	$C_{14}D_{30}$
c_d, J/(kg K)	1780	1652.9	2768	2404
$e_d^{(ch)}$, J/kg	29.27×10^6	27.18×10^6	40.53×10^6	35.2×10^6
$e_i^{(ch)}$, J/kg	7.72×10^9	7.18×10^9	7.2×10^9	6.266×10^9
e_d°, J/kg	1.4589×10^6	1.3547×10^6	1.7054×10^6	1.4810×10^6
ρ_{L0}, kg/m^3	879	946.6	763	878.6
ρ_d°/ρ_{L0}	1.4045		1.3057	
A_d, Pa	0.35×10^8		0.2×10^9	
b_d	13.7		11.5	
K_d, Pa	0.4×10^9		1.0×10^9	
ξ_d	0.3333		0.3333	
β_d	0.6666		0.6666	

$$H_2 = [(H + H) + Q_{H_2}] \text{ or } D_2 = [(D + D) + Q_{D_2}].$$

Next, the hidden energy required for the complete dissociation of unit mass of a relevant substance in the gas phase into relevant atoms was obtained (Table 3). For benzene, it is as follows:

$$\begin{aligned} e_d^{(ch)}(C_6H_6) &= 1/78\left[Q_m + 3Q_{H_2}\right] \\ &= 29.27\times10^6 \text{ J/kg}, \\ e_d^{(ch)}(D_6H_6) &= 1/84\left[Q_m + 3Q_{D_2}\right] \\ &= 27.18\times10^6 \text{ J/kg}. \end{aligned} \tag{14}$$

The ionization energy, $e_i^{(ch)}$, was calculated based on the bond energies of all Z-type electrons of the corresponding molecule by the analogy with [1]. The benzene molecule has one electron in each of the six deuterium (j = D1) or hydrogen (j = H1) atoms, and six electrons in each of the six carbon atoms (j = C1, C2, C3, C4, C5, C6). Each of these (Z = 7)-type electrons in one molecule of benzene with Z_e = 42 (Z_e = 6 × 6 + 6 × 1 = 42) has its own bond energy, $\varphi_j \equiv k_B T_j$ (j = 1, 2, ... , Z = 7), which is determined by the ionization temperature, T_j, and the Boltzmann constant, k_B [23]. The ionization level, x_j, is an ionization part of the j-th type of electrons, and ν_j is the number of atoms in a molecule at appropriate ionization levels, which is equal, for example, to $\nu_D = \nu_{D1} = \nu_{H1} = 6$, $\nu_C = \nu_{C1} = \nu_{C2} = ... = \nu_{C6} = 6$ in the case of C_6D_6 or C_6H_6. Hence, the chemical component of the internal ionization energy for C_6D_6 is reduced to the following form:

$$\begin{aligned} e_i^{(ch)} &= \sum_{j=1}^{Z} \frac{N_A \nu_j}{M} x_j \varphi_j \\ &= \frac{R}{M}\left\{6T_{D1}x_{D1} + 6\sum_{j=C1}^{C6} T_j x_j\right\}, \end{aligned} \tag{15}$$

where N_A is the Avogadro number.

The ionization temperatures, T_j, of electrons in eV (1 eV = 11.604.5 K), which are used in Eq. (15), are taken from [23]:

$$\begin{gathered} T_{H1} = 12.60, \quad T_{D1} = 13.60, \quad T_{C1} = 11.26, \\ T_{C2} = 23.38, \quad T_{C3} = 47.89, \quad T_{C4} = 64.49, \\ T_{C5} = 392.0, \quad T_{C6} = 490.0. \end{gathered}$$

Thus, the full ionization energies for all the studied substances are obtained (Table 3). The evaluation of the temperature corresponding to the full ionization energy ($T_i \approx e_i^{(ch)}/c$) shows that the dissociation and ionization processes may be completed when the temperature is no less than 10^7 K. Nevertheless, partial dissociation and ionization during the processes occurring at lower temperatures (heat transfer, evaporation, condensation, etc.) also play a role in the gas-dynamics calculations. In order to make an allowance for these partial processes, the mass fractions, x_d, of dissociated phases from Eq. (12), which are determined by a particular form of the function, x_d, for example, by the linear kinetic equation used in [1], are introduced as depending on the dissociation (T_d) or ionization (T_j) temperatures, and on the relaxation time, τ_j:

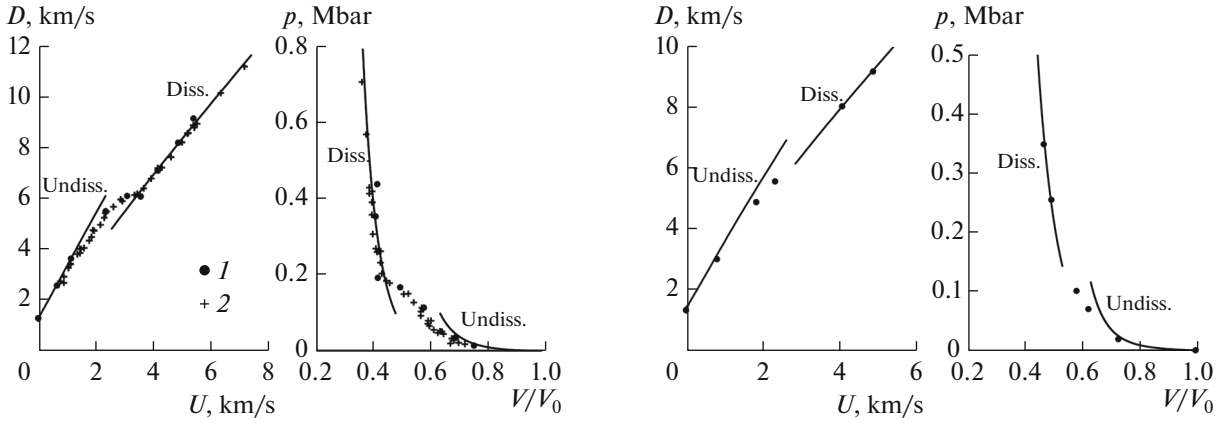

Fig. 1. Shock adiabats of (a) benzene and (b) tetradecane in the U–D and p–V/V_0 coordinates; undiss. designates an undissociated phase and diss. a dissociated phase; (*1*) experimental data from [25] and (*2*) from [26].

$$\frac{dx_j}{dt} = x_{j^*}\frac{T - T_j}{T_j}\frac{1}{\tau_j}, \tag{16}$$

where $x_{j^*} = x_{j-1}$ at $T \geq T_j$; and $x_{j^*} = x_j$ at $T < T_j$ ($0 \leq x_j \leq 1$, $j = m, d, 1, 2, \ldots, Z$). The relaxation time can vary in the range from 10^{-12} to 5×10^{-9} s [1].

The model introduced with Eqs. (1)–(10), (12), (15), and (16) provides a continuous transition from the undissociated molecular to dissociated states, then to the ionized state by moving from the equations of state for a molecular gas/vapor ($k = m$) to the equations of state for dissociated and ionized gases.

The problem is in determining the potentials given in Eqs. (3) and (4) for the molecular and dissociated phases. The two different approximations of the elastic potential from Eqs. (3) and (4) are used here: the first one ($p_m^{(p)}$, $e_m^{(p)}$) with the coefficients, A_d, b_d, β_d, K_d, and ξ_d, differing by the Grünaisen function and heat capacities for the liquid (G_L, c_L) and gaseous (G_G, c_G) in accordance with Eq. (6), is used for the molecular liquid and gaseous phases; the second approximation of the elastic potential ($p_d^{(p)}$, $e_d^{(p)}$) is used for the dissociated state with the A_d, b_d, β_d, K_d, and ξ_d coefficients, Grünaisen coefficient (G_d), and heat capacity (c_d), and for all the ionized states in keeping with Eqs. (1)–(4) and (7), and with the parameters obtained using Eqs. (13)–(15) (Table 3).

EQUATION OF STATE AT HIGH DENSITIES AND PRESSURES

The experimental data on the studied substances under shock [25, 26] and isothermic compressions [11, 12], as well as the data on the pressure and heat of vaporization at the saturation line of liquid and vapor [11, 12, 22, 23], and theoretical approximations based on the Thomas–Fermi model with quantum and exchange corrections (TFC) [27], were used for description of the behavior of substances under strong compression (liquid or vapor phases) and for large volumes (vapor phase), i.e., for determining the values of unknown parameters in Eqs. (1)–(6).

Let us analyze the Hugoniot shock adiabat, which follows from the laws of mass, momentum, and energy conservation on the shock jump [16–18], expressed as follows:

$$\rho_{L0}D = \rho(D - U), \quad \rho_{L0}DU = p - p_0,$$
$$\rho_{L0}D\left(e + 1/2U^2 - e_0\right) = pU. \tag{17}$$

In this, ρ_{L0}, p_0, and e_0 and ρ, p, and e, are the density, pressure, and internal energy before (index 0) and after (without index) the shock jump, respectively; D and U are the shock wave velocity and mass velocity of the particles of a medium behind the shock wave, respectively. The velocities are calculated from a state of rest in front of the shock front, i.e., $U_0 = 0$.

In the experiments with condensed media (solids and liquids), the shock wave velocity (D) and mass velocity behind the shock wave (U) were measured for various shock wave strengths in different substances. It is possible to calculate the shock adiabat, $D(U)$, of a substance on the basis of experimental data. Using the conservation laws Eq. (17) and experimental data on the dependence, $D(U)$, of the shock front velocity on the mass velocity of a substance, the dependence, $p(\rho)$, characterizing the shock compressibility can be calculated [25, 16–18]. The line approximating the shock adiabat, $D(U)$, for condensed substances is straight:

$$D = C_0 + k_0 U,$$

where C_0 is the speed of sound, k_0 is the slope of the shock adiabat. The slope, k_0, changes for some substances, and a transition into another straight line occurs [13, 25]. This is connected with the physical and chemical transformations (i.e., phase transitions that change the crystal structure, chemical reactions, dissociation of molecules, etc.) caused by the strong

shock wave compression and heating. For hydrocarbon liquids, in particular benzene and tetradecane, the experimental dependence of the shock front velocity, D, on the mass velocity, U, of particles behind the shock wave front was measured in [25, 26], which is shown in Fig. 1 by dots. A change in the slope is seen in the diagrams at $U > 2$ km/s, which corresponds to a shock compression pressure of $p > 60$ kbar. The reason for this change of the slope is a chemical transformation, namely, the dissociation of a molecule, i.e., its collapse into the atomic state. Let us note here, that the phase transitions caused by shock waves are characterized by relaxation time [16, 18] of about $\tau_d > 10^{-7}$ s. The shock adiabats at a low shock wave intensity of $U < 2.0$ km/s ($p < 60$ kbar) in Fig. 1 correspond to undissociated liquids. The straight line at higher intensities ($U > 4.0$ km/s and $p > 200$ kbar) is related to the dissociated phase. The intermediate points ($1.8 < U < 4.0$ km/s and $61 < p < 200$ kbar) correspond to the partial dissociation of molecules in the shock wave. Two lines of the shock adiabats, $p_{sh}(\rho)$, for the studied substances in the undissociated and dissociated phases (with the following initial conditions in front of the shock wave: $p_0 = 1$ bar and $T_0 = 293$ K) are shown in Fig. 1 by solid lines. The theoretical shock adiabat, $p_{sh}(\rho)$, can be obtained from the shock wave conservation laws Eq. (17) and equations of state in the form of Eqs. (3)–(6), giving rise to the following equation [16, 18]:

Table 4. Approximation constants of the Grünaisen function

Constant	Benzene	Tetradecane
$a^{(0)}$	14.5792	29.306
$a^{(1)}$	6.0495	36.979
$a^{(2)}$	7.3557	13.964
$\rho^{(0)}/\rho_{L0}$	1.2931	1.600
$\rho^{(1)}/\rho_{L0}$	1.0676	1.225
$\rho^{(2)}/\rho_{L0}$	1.0279	1.0462
$\alpha^{(0)}$	1.75	1.4
$\alpha^{(1)}$	–2.4	–2.0
$\alpha^{(2)}$	–9.3	–14.0

$$p_{sh}(\rho) = \frac{\frac{2}{G(\rho)}p^{(p)}(\rho) + p_0\left(\frac{\rho}{\rho_{L0}} - 1\right) - 2\rho\left(e^{(p)}(\rho) + e^{(ch)} - e_0\right)}{1 + \frac{2}{G(\rho)} - \frac{\rho}{\rho_{L0}}}. \quad (18)$$

For the molecular gas and liquid phases described by EOS, which are uniform in regards to the pressure and different in regards to the heat capacity and Grünaisen function expressed by Eqs. (4)–(6), the isochoric pressure coefficient, $\xi_V(\rho)$, is approximated in the following form:

$$\frac{\xi_V(\rho)}{\rho} = G(\rho)c_V = \frac{R}{M}\left(a^{(0)} + \left(1 - a^{(0)}\right) \times \exp\left(-\left(\frac{\rho}{\rho^{(0)}}\right)^{\alpha^{(0)}}\right) + a^{(1)}\exp\left(-\left(\frac{\rho}{\rho^{(1)}}\right)^{-\alpha^{(1)}}\right) + a^{(2)}\exp\left(-\left(\frac{\rho}{\rho^{(2)}}\right)^{-\alpha^{(2)}}\right)\right).$$

Here, $a^{(0)}$, $a^{(1)}$, $a^{(2)}$, $\rho^{(0)}$, $\rho^{(1)}$, $\rho^{(2)}$, $\alpha^{(0)}$, $\alpha^{(1)}$, and $\alpha^{(2)}$ are the constants given for the studied substances in Table 4.

Knowing the state at the standard conditions ($T = T_0 = 293$ K, $p = p_0 = 10^5$ Pa, $\rho = \rho_{L0}$, and C_{L0}) (Table 1) and the equation of the adiabatic speed of sound [18], the following expressions are obtained with the use of Eqs. (3)–(6) for determining the parameters, A, K, b, $G(\rho_{L0})$, and $G'(\rho_{L0}) = \partial\Gamma/\partial\rho\big|_{\rho=\rho_{L0}}$:

$$C_{L0}^2 = \frac{A}{\rho_{L0}}(\beta(b-1)+1) - c_{L0}T_0\left(G_0^2 + G_0'\rho_{L0} - \xi G_0\right) + \frac{p_0}{\rho_{L0}}(\xi + 1),$$

$$A - K + \rho_{L0}G(\rho_{L0})c_{L0}T_0 = p_0.$$

The following conditions are used at the critical point:

$$p_{cr} = p(\rho_{cr}, T_{cr}), \quad \left(\frac{\partial p}{\partial \rho}\right)_T = 0, \quad \left(\frac{\partial^2 p}{\partial \rho^2}\right)_T = 0.$$

Consequently, the problem of the formulation of EOS for the molecular liquid–vapor phase is reduced to determination of the coefficients, which conform the experimental and calculated data on the shock (Fig. 1) and isothermic (Figs. 2–4) compressibilities, the saturation pressure $p_S(T)$, and the heat of vaporization, $h_{LG}(T)$, according to Eqs. (9)–(11) (Fig. 5). These coefficients were calculated through minimization of the standard deviation of the shock compression pressure, $p_{sh}(\rho)$, found from Eq. (18), the theoretical isotherms near the critical point, and the saturation line, $p_S(T)$, determined by Eq. (10) from the corresponding experimental data. The calculated $p(\rho, T)$

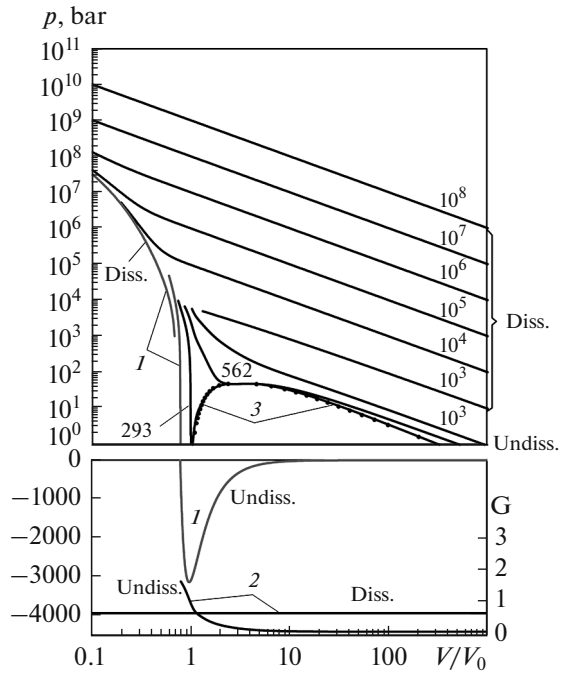

Fig. 2. Calculated isotherms of benzene in the undissociated liquid, gas, and dissociated phases; curve (*1*) corresponds to $p^{(P)}$, (*2*) to G, and (*3*) to the saturation line; numbers at the curves indicate temperatures in K.

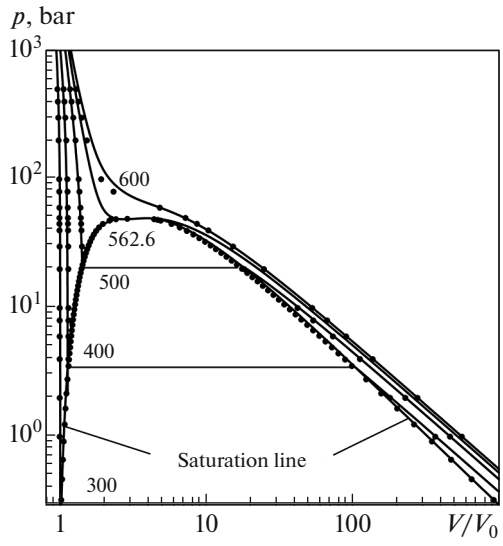

Fig. 3. Calculated isotherms of benzene in the undissociated liquid and gas phases at the subcritical region; dots designate experimental data from [11]; numbers at the curves indicate temperatures in K.

isotherms for undissociated and dissociated liquids at different temperatures are given in Figs. 2–4. It should be noted here that the isotherm at $T = 0$ K is related the potential (cold) pressure, $p^{(P)}(\rho)$, of the dissociated and undissociated states. For the molecular phase of benzene, more detailed comparison of the theoretical

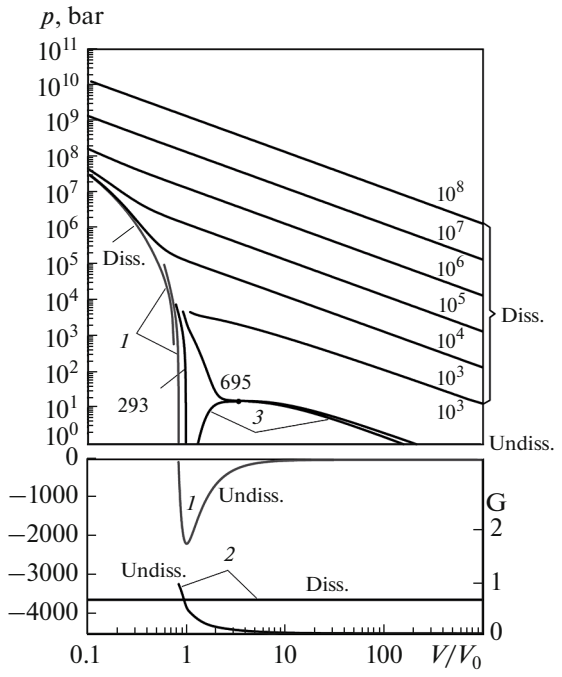

Fig. 4. Calculated isotherms of tetradecane in the undissociated liquid, gas, and dissociated phases; designations are the same as in Fig. 2.

liquid and gas isotherms, and the saturation line $p_S(\rho)$ in the subcritical area with the experimental data from [11] is given in Fig. 3. A comparative analysis of the experimental and theoretical data showed that the relative errors, $\delta_{p_S(T)}$ and $\delta_{h(T)}$, of the approximation of the experimental data [11, 22] at the saturation line in the temperature dependences of the saturation pressure, $p_S(T)$, and the vaporization heat, $h^*_{LG}(T)$, for benzene and tetradecane do not exceed 0.1% (see Fig. 5). The relative errors of the experimental data on the heat of vaporization and the $h_{LG}(T)$ dependences calculated by Eq. (9), which are obtained with the use of equations of states constructed in the present studies for benzene and tetradecane, do not exceed 3% (see Fig. 5b). The relative error, $\delta_{p_S(T)}$, of the available experimental data for benzene in the form of the dependence of the saturation pressure on the density of liquid ($p_S(\rho_{LS})$) and gas ($p_S(\rho_{GS})$) phases at the saturation line and the calculated data obtained with the use of the constructed equation of state is less than 3% (see Fig. 3). The accuracy can be increased by using more detailed and complex approximations.

Appropriate parameters for $e_m^{(P)}(\rho)$ and $p_m^{(P)}(\rho)$ of molecular (undissociated) gas and liquid phases are summarized in Table 1. For each state of the studied substances, namely, liquid ($j = L$) and gas ($j = 1, 2, ..., Z$) phases, the potential summands for $p^{(P)}(\rho)$ and $e^{(P)}(\rho)$ are substantial only for high densities ($\rho/\rho_{L0} > 0.1$),

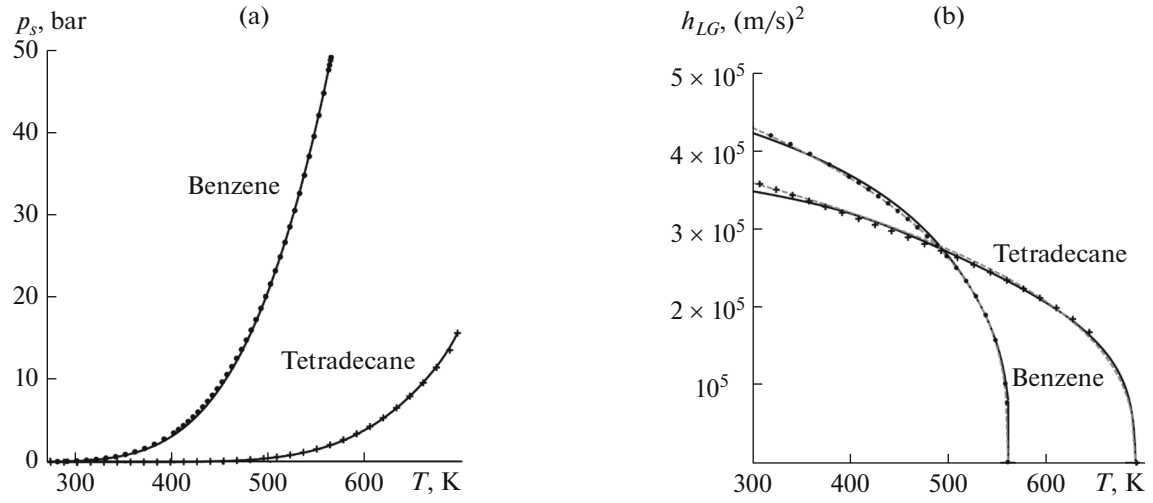

Fig. 5. Approximations of experimental data for the (a) saturated vapor pressure, $p_s(T)$, (b) (dashed line) vaporization enthalpy, $h^*_{LG}(T)$, and (solid line) vaporization enthalpy, $h_{LG}(T)$, calculated by Eq. (9) of benzene and tetradecane; dots designate experimental data from [11, 22].

whereas for low densities and high temperatures ($T > 10^3$ K) $p^{(P)} \ll p^{(T)}$. In this regard, the coefficients of the elastic potential for the dissociated and ionized states can be calculated using the straight line of the shock adiabat corresponding to the densities ($\rho/\rho_{L0} > 1$) of the dissociation area (Figs. 1, 2, and 4). Regardless of the ionization degrees, x_j, the elastic potential coefficients for the dissociated gas state ($k = d$) are calculated using the theoretical concepts based on the self-similar Thomas–Fermi theory [27], in which an extrapolation can be applied for obtaining the correct asymptotics of the elastic pressure $p^{(P)} \sim \rho^{5/3}$ under high compressions; the results are given in Table 3.

CONCLUSIONS

On the example of conventional (H-) hydrocarbon liquids, namely, benzene and tetradecane, and their deuterated (D-) analogues, common analytic EOS for liquid and gas states in the broad range of pressures ($p \le 1000$ bar) and densities ($\rho/\rho_0 \le 1.5$) of the molecular phase are constructed in the form of Mie–Grünaisen relations based on the proposed procedures. The constructed equations of state transform into EOS of the ideal gas in the area of low densities and pressures. They take into account the behavior of a substance at the saturation line in the vicinity of the critical point, agree with the experimental data on the shock compression, and describe the dissociation and ionization processes proceeding under super-high compressions ($\rho/\rho_0 < 10$) and temperatures up to 10^8 K. The obtained theoretical dependences of the equation of state for the investigated substances and the experimental data complying with them are shown in Figs. 1–5. A nonequilibrium scheme is used for calculations in the area of ultrahigh energy densities, and a more detailed analysis of the effects of dissociation, ionization, and shell electronic structure of atoms [9, 28] might be required in further studies.

ACKNOWLEDMENTS

This work was supported by the Russian Foundation for Basic Research (project nos. 14-01-97007 and 14-01-97014 r_povolzh'ye_a) and by the Council on President's Grants of the Russian Federation within Program for State Support of Leading Scientific Schools of the Russian Federation (project no. NSh- 6987.2016.1).

REFERENCES

1. Nigmatulin, R.I., Akhatov, I.Sh., Topolnikov, A.C., Bolotnova, R.Kh., Vakhitova, N.K., Lahey, Jr.R.T., and Taleyarkhan, R.P., *Phys. Fluids*, 2005, vol. 17, no. 10, 107106.
2. Nigmatulin, R.I., Aganin, A.A., Il'gamov, M.A., and Toporkov, D.Yu., *J. Appl. Mech. Tech. Phys.*, 2014, vol. 55, no. 3, p. 82.
3. Nigmatulin, R.I., Lahey, R.T., Jr., Taleyarkhan, R.P., Vest, K.D., and Blok, R.S., *Phys.—Usp.*, 2014, vol. 57, no. 9, p. 877.
4. Son, E.E., *High Temp.*, 2013, vol. 51, no. 3, p. 351.
5. Stankus, S.V., Khairulin, R.A., Martynets, V.G., and Bezverkhii, P.P., *High Temp.*, 2013, vol. 51, no. 5, p. 695.
6. Anderko, A., *Fluid Phase Equilib.*, 1990, vol. 61, nos. 1–2, p. 145.
7. Wei, Y.S. and Sadus, R.J., *J. Am. Inst. Chem. Eng.*, 2000, vol. 46, no. 1, p. 169.
8. Bushman, A.V., Lomonosov, I.V., Fortov, V.E., and Khishchenko, K.V., *Khim. Fiz.*, 1994, vol. 13, no. 5, p. 97.
9. Fortov, V.E., *Phys.—Usp.*, 2007, vol. 50, no. 4, p. 333.

10. Sapozhnikov, A.T., Gershchuk, P.D., Malyshkina, E.L., Mironova, E.E., and Shakhova, L.N., *VANT, Ser. Mat. Model. Fiz. Protsessov*, 1991, no. 1, p. 9.
11. Vargaftik, N.B., *Spravochnik po teplofizicheskim svoistvam gazov i zhidkostei* (Handbook of Thermophysical Properties of Gases and Liquids), Moscow: Fizmatgiz, 1972.
12. Beaton, C.F. and Hewitt, G.F., *Physical Property Data for the Design Engineers*, New York: Hemisphere, 1989.
13. Trunin R.F., *Phys.—Usp.*, 2001, vol. 44, no. 4, p. 371.
14. Nigmatulin, R.I. and Bolotnova, R.Kh., *Dokl. Phys.*, 2007, vol. 52, no. 8, p. 442.
15. Nigmatulin, R.I. and Bolotnova, R.Kh., *High Temp.*, 2011, vol. 49, no. 2, p. 303.
16. Zel'dovich, Ya.B. and Raizer, Yu.P., *Fizika udarnykh voln i vysokotemperaturnykh gidrodinamicheskikh yavlenii* (Physics of Shock Waves and High-Temperature Hydrodynamic Phenomena), Moscow: Nauka, 1966.
17. Zharkov, V.N. and Kalinin, V.A., *Uravneniya sostoyaniya tverdykh tel pri vysokikh davleniyakh i temperaturakh* (The Equations of State of Solids at High Pressures and Temperatures), Moscow: Nauka, 1968.
18. Nigmatulin, R.I., *Dinamika mnogofaznykh sred* (Dynamics of Multiphase Media), Moscow: Nauka, 1987, part 1.
19. Nigmatulin, R.I., *Mekhanika sploshnoi sredy. Kinematika. Dinamika. Termodinamika. Statisticheskaya dinamika* (Continuum Mechanics. Kinematics. Dynamics. Thermodynamics. Statistical Dynamics), Moscow: GEOTAR-Media, 2014.
20. Jacobs, S.J., *On the Equation of State of Compressed Liquids and Solids NOLTR 68–214, United States Naval Ordnance Laboratory*, Maryland: White Oak, 1968.
21. Taleyarkhan, R.P., West, C.D., Cho, J.S., Lahey, R.T., Jr., Nigmatulin, R.I., and Block, R.C., *Science*, 2002, vol. 295, p. 1868.
22. *NIST Chemistry WebBook, NIST Standard Reference Database*, Linstrom, P.J. and Mallard, W.G., Eds., Gaithersburg, MD: Natl. Inst. Stand. Technol., 2014, no. 69. http://webbook.nist.gov.
23. *Fizicheskie velichiny. Spravochnik* (Physical Quantities: Handbook), Grigor'ev, I.S., Meilikhov, E.Z., Eds., Moscow: Energoatomizdat, 1991.
24. Gordon, A. and Ford, R., *The Chemist's Companion: Handbook of Practical Data*, New York: Interscience, 1972.
25. Trunin, R.F., Zhernokletov, M.V., Kuznetsov, P.F., and Sutulov, Yu.N., *Khim. Fiz.*, 1989, vol. 8, no. 4, p. 539.
26. Nellis, W.J., Ree, F.H., Trainor, R.J., Mitchell, A.C., and Boslough, M.B., *J. Chem. Phys.*, 1984, vol. 80, no. 6, p. 2789.
27. Kalitkin, N.N. and Kuz'mina, L.V., Tables of thermodynamic functions of substances at a high concentration of energy, *Preprint of the Inst. Appl. Math., USSR Acad. Sci.*, Moscow, 1975, no. 3.
28. Fortov, V.E. and Yakubov, I.T., *Neideal'naya plazma* (Nonideal Plasma), Moscow: Energoatomizdat, 1994.

Translated by O. Kadkin